J 24

PREDICTION OF FORCES IN OBLIQUE CUTTING

P. K. Venuvinod* and W. L. Jin**

ABSTRACT

The material at the lower boundary of the primary deformation zone in cutting should, by definition, have experienced no cutting deformation. Hence the shear flow stress on the lower boundary must be a work material constant. Thus, modelling of orthogonal cutting based on the lower boundary has been particularly successful in predicting the power component of the cutting force when continuous chips without built up edge are produced. This paper extends this approach to oblique cutting. It is assumed that the progressive deformation of the work material into chip material occurs within a plane called the deformation plane. An application of plasticity theory shows that certain simplifying assumptions concerning the three dimensional stress distribution on the lower boundary can be made with acceptable accuracy. The resulting stress distributions on the lower boundary are then integrated to yield expressions for estimating cutting forces from given tool and chip geometries. It is noted that force components parallel to the cutting plane may be estimated by assuming that the deformation plane is parallel to the "effective plane", i.e. the plane parallel to the initial work velocity and the final chip velocity. This provides a mechanism for predicting the power and lateral components of the cutting force. The third force component, namely the thrust force component, may then be predicted from the condition of collinearity between the chip velocity and the direction of the friction force at the chip/tool interface. The predictions are verified against new and previously published experimental data from oblique cutting.

Nomenclature

A_m	area of Merchant shear plane (P_m)
$\mathbf{A}_m$	area vector of Merchant shear plane, i.e. vector with magnitude equal to A_m and directed perpendicular to P_m (directed towards chip material)
b	workpiece width
C	a constant related to the normal stress distribution on the TLB
dA	an area element on the lower boundary of the primary deformation zone
$\mathbf{dA}$	area vector of dA, i.e. a vector with magnitude equal to the area of dA and directed normal to dA
df_j	contribution to f_j due to deformation at dA
f_l	cutting force component parallel to the cutting edge
f_c	cutting force component in the direction of V
f_{cn}	cutting force component parallel to P_s and perpendicular to the cutting edge
f_j	cutting force vector in direction j
f_l	cutting force component parallel to P_s and perpendicular to V
f_v	cutting force component perpendicular to P_s

* Professor, Dept of Manufacturing Eng., City Polytechnic of Hong Kong

** Associate Professor, Nanjing Aeronautical Institute, Nanjing

i angle of inclination of the cutting edge, i.e. the angle between $\boldsymbol{V}$ and P_n (ISO λ_s)

s shear flow stress of unmachined work material (a work material property)

t_1 undeformed chip thickness

t_2 chip thickness

p mean normal stress on the segment of the lower boundary of the primary deformation zone which is not coincident with P_s

p_m mean normal stress on the segment of the lower boundary of the primary deformation zone which is coincident with P_s

P_d plane in which the progressive deformation of an element of work material into the corresponding chip element is assumed to occur

P_{ef} plane parallel to $\boldsymbol{V}$ and $\boldsymbol{V}_c$

P_{dA} normal stress on dA

P_m 'Merchant' shear plane, i.e., the plane passing through the cutting edge and the line of intersection between the initial work surface and the chip surface

P_n 'normal' plane, i.e. the plane perpendicular to the cutting edge (and rake face) (ISO)

P_s tool cutting edge plane, i.e. the plane containing the cutting edge and $\boldsymbol{V}$ (ISO)

$\boldsymbol{u}_{dA}$ unit vector normal to dA

$\boldsymbol{u}_{nd}$ unit vector perpendicular to P_d

$\boldsymbol{u}_{nef}$ unit vector perpendicular to P_{ef}

$\boldsymbol{u}_j$ unit vector parallel to an arbitrary direction j

$\boldsymbol{u}_m$ unit vector perpendicular to P_m (directed towards chip material)

$\boldsymbol{u}_{Vs}$ unit vector parallel to $\boldsymbol{V}_s$

V, $\boldsymbol{V}$ magnitude of cutting velocity and cutting velocity vector (towards the cutting edge) respectively

V_c, $\boldsymbol{V}_c$ magnitude of chip velocity and chip velocity vector (away from the cutting edge) respectively

V_s, $\boldsymbol{V}_s$ magnitude of shear velocity and shear velocity vector (towards the cutting edge) respectively on P_m ($\boldsymbol{V}_s = \boldsymbol{V} - \boldsymbol{V}_c$)

V_x, V_y, V_z velocity components of a material element parallel to axes x, y and z respectively

α_n 'normal' rake angle, i.e. the rake angle measured in P_n (ISO γ_n)

η_c chip flow angle, i.e. the angle between $\boldsymbol{V}_c$ and the line of inetrsection between the rake face and P_n

η_s acute angle between the shear velocity at a point along the lower boundary of the shear zone and P_n when measured in the plane tangent to the lower boundary at the point

η_{sB} magnitude of η_s at the junction between chip and unmachined work surfaces

η_{sB}^* angular deviation from P_n to the line of intersection between P_{ef} and the lower boundary of the primary deformation zone where the latter meets the unmachined work surface.

η_{sm} acute angle between $\boldsymbol{V}_s$ and the line of inetrsection between P_m and P_n

θ_{dA} acute angle between $\boldsymbol{u}_{dA}$ and $\boldsymbol{u}_{nd}$ (or, $\boldsymbol{u}_{nef}$)

θ_1, θ_2 magnitudes of θ_{dA} for to planes 1 and 2 respectively in Fig. 2b

ϕ_n 'normal' shear angle, i.e. the acute angle between P_m and P_s

ϕ_e 'effective' shear angle, i.e. the acute angle between $\boldsymbol{V}$ and $\boldsymbol{V}_s$

ψ_n acute angle between the plane tangential to the lower boundary of the primary deformation zone (at a given point) and P_s

ψ_{nB} magnitude of ψ_n at the junction between chip and unmachined work surfaces

λ apparent friction angle at the tool/chip interface

σ_m	mean normal stress in a material element
σ_x, σ_y, σ_z	'normal' stresses on area elements perpendicular to axes x, y and z respectively
σ_θ	normal stress on an area element parallel to axis x and inclined at angle θ to plane xy in Fig. 3
τ	mean shear stress on the Merchant shear plane, P_m
τ_{xy}, τ_{yz}, τ_{xz}	shear stresses on area elements parallel to planes containing axes (x, y),(y, z) and (x, z) respectively
$\tau_{x\theta}$, $\tau_{y\theta}$	shear stresses on a plane parallel to axis x and inclined at angle θ to xy plane
$\dot{\epsilon}_x$, $\dot{\epsilon}_y$, $\dot{\epsilon}_z$	'normal' strain rates on area elements perpendicular to axes x, y and z respectively
$\dot{\epsilon}_{xy}$, $\dot{\epsilon}_{yz}$, $\dot{\epsilon}_{xz}$	shear strain rates on area elements parallel to planes containing axes (x, y), (y, z) and (x, z) respectively

Other symbols used are defined in the text of the paper.

1. INTRODUCTION

A cutting operation in which the cutting speed vector, V, deviates from the plane normal to the cutting edge, P_n, is said to be oblique. Chip formation and cutting mechanics in such operations tend to be three dimensional. Since a vast majority of cutting operations in practice are oblique to some degree, the prediction of cutting forces in such operations is a problem of practical significance.

Classical models of oblique cutting [1 and 2] resulting in continuous chip formation without built up edge, have been based on the utilisation of the notion of Merchant shear plane. In these models the prediction of any of the three cutting force components requires *a priori* knowledge of the mean shear stress, τ, on the shear plane and the apparent friction angle, λ, at the tool/chip interface in addition to that of chip geometry. Unfortunately, both τ and λ happen to depend on cutting conditions in addition to the tool/work material pair which often means that they cannot be known *a priori*. Thus, models based purely on the "Merchant" shear plane have been unable to *predict* any of the cutting force components even in the two dimensional case of orthogonal cutting (when $i=0$).

In contrast, the analysis of orthogonal cutting based on the lower boundary of the shear zone, as proposed by Connolly and Rubenstein [3 and 4], has been able to predict the power component, f_c, of the cutting force merely from known magnitudes of the shear flow stress, s, of the work material and the chip thickness. This has been possible because the magnitude of s is a property of the work material prior to being subjected to any cutting deformation so that, unlike τ, s must be a true material constant.

Previous attempts to extend the lower boundary concepts, which have proved highly successful in orthogonal cutting [3 and 4], to oblique cutting (for example, as in [5]), had relied on intuitive definitions concerning the geometry of and the stress distributions on the lower boundary. The present paper aims to present a more rigorous approach towards extending the fundamental notions behind Rubenstein's model of orthogonal cutting [4] to the case of oblique cutting.

2. THE LOWER BOUNDARY OF THE PRIMARY DEFORMATION ZONE IN ORTHOGONAL CUTTING

Consider Fig. 1 which illustrates Rubenstein's model of orthogonal cutting [4]. Curve DTCB represents the true lower boundary (TLB) of the primary deformation zone whereas straight line DB represents the Merchant shear plane. Basing his arguments on the plasticity conditions near B, Rubenstein noted that, at B, the TLB must meet the unmachined work surface at 45° and the normal stress on the TLB should be equal to the shear stress, s, which must be uniformly distributed over the TLB [4]. Likewise, on the basis of the condition of chip/work material separation, it was noted that the TLB must be parallel to the tool cutting edge plane, P_s, in the vicinity of D. Further, following a rigorous application of translational equilibrium criteria to the tool/chip/primary deformation zone/workpiece system, Rubenstein made the following observations: "Provided the stresses (normal stress, p, and shear stress, s) are uniformly distributed, the force components f_c (parallel to the cutting speed) and f_v (parallel to the normal to the machined surface) are *path independent*, i.e. along any boundary joining B and D, including the Merchant shear plane, the same force components will be obtained when the magnitudes of the stresses (p and s) are specified. Of the infinity of paths joining B and D, one of these is the TLB. The force components acting on the TLB may be determined by calculating the force components along an arbitrarily chosen boundary joining the extremeties of the TLB provided (i) the stresses which are assumed to act on the arbitrarily chosen boundary are the same as those acting on the TLB, and (ii) the stresses are uniformly distributed" [4].

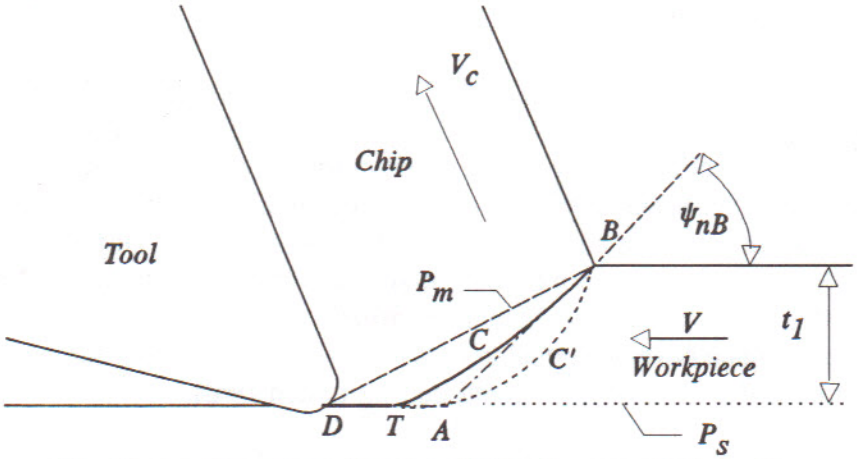

The Figure shows a section parallel to the normal plane, P_n

DB : Merchant Shear Plane
DAB : Assumed Path of Planes (AB : Plane 1, DA : Plane 2)
DTCB : True Lower Boundary
DTC'B : Assumed Boundary Partly Overlapping the TLB

Fig. 1 The lower Boundary of the Shear Zone in Orthogonal Cutting

Rubenstein next observed that if the assumed boundary (DTC'B) had a segment (TD) coincident with the TLB (DTCB) and the TLB is subjected, in its non-coincident segment, to uniformly distributed stresses, the force components calculated by integrating over the assumed boundary will be the same as those calculated by integrating over the TLB, irrespective of whether or not the assumed boundary has any physical significance (see Fig. 1) [4].

Based on this premise, Rubenstein chose an assumed boundary represented by planes DA and AB which are tangential to the TLB at the latter's extremities D and B respectively. Following the above arguments, (i) the shear stress on DA and AB were taken to be uniformly distributed with its magnitude equal to s, (ii) the normal stress on AB was taken to be uniformly distributed and equal to s, and (iii) the normal stress on DA was taken to be of unknown distribution and magnitude. Integration of these stresses over path DAB yielded the following equation for estimating f_c which is a function of just s, the uncut area ($= bt_1$), and the shear angle, ϕ_n.

$$f_c = sbt_1(cot\phi_n + 1) \tag{1}$$

This equation has been shown to be quite accurate and robust in the light of extensive experimental data obtained in orthogonal cutting conditions [3].

3. ASSUMPTIONS

The following assumptions are made in developing the new model of oblique cutting :

A1. The cutting tool is perfectly sharp.
A2. The work material is a perfectly plastic and isotropic continuum.
A3. Chip formation is of type 2 (continuous chip with no built up edge present).
A4. The chip is a rigid body in equilibrium under the action of the forces exerted on it from the primary deformation zone and the chip/tool interface at the tool rake.
A5. On the rake face, the tangential force at the chip/tool interface is collinear with the chip velocity vector, $\mathbf{V}_c$.
A6. The nature of chip deformation is identical in any section normal to the cutting edge.
A7. The primary deformation shear zone is thin, i.e. its thickness is substantially smaller than its length.
A8. The progressive deformation of an element of work material into the corresponding element in the chip material occurs within a plane which we will call the deformation plane, P_d .(The orientation of P_d is unknown at this stage of the analysis. However, further analysis will be directed towards identifying this plane.)

4. THE TLB IN OBLIQUE CUTTING

We now examine how the basic notions contained in Rubenstein's model of TLB in orthogonal cutting [4] may be extended to single edge oblique cutting. Fig. 2a illustrates the proposed approach. Plane B'B"D"D' is the Merchant shear plane. The TLB is a curved surface joining B'B" and D'D". As in [4], the TLB is assumed to (i) be tangential to the cutting plane in the vicinity of the cutting edge and (ii) meet the unmachined work surface at the other end, B'B", at angle ψ_{nB} when measured in the plane normal to the cutting edge. Thus, in Figure 2, segment D'D"T"T' of the TLB is coincident with the cutting plane, P_s. The exact geometry of the non-coincident segment, B'B"T"T', is however unknown. Following assumption A8, the curve of intersection DTB between the TLB and the deformation plane, P_d (as yet unidentified), is taken to represent the direction of shear along the TLB.

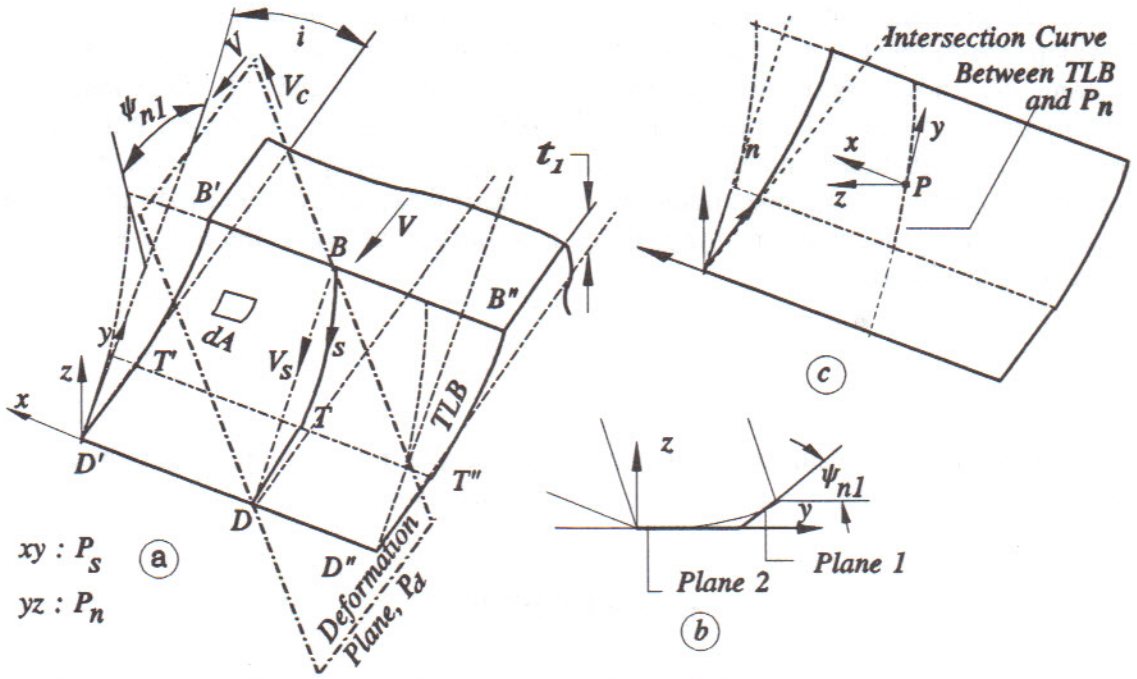

Fig. 2 The Lower Boundary of the Primary Deformation Zone in Oblique Cutting

Consider an area element of area dA located on the TLB (see Fig. 2a). Let u_{dA} be the unit vector normal to the area element. As in [4], we assume that the shear stress is the same at every location on the TLB and has its magnitude equal to the shear flow stress, s, of the unmachined work material. In contrast, the normal stress could be variable across the TLB. Let p_{dA} be the normal stress on dA. Clearly, p_{dA} acts in the direction of u_{dA} so that $p_{dA}(dA)u_{dA}$ is the vector representing the normal force on dA. The shear stress is *assumed* to be directed along the line of intersection of the deformation plane, P_d, with the area element. Thus the shear force vector on dA is given by $s(dA)\{(u_{dA} \times u_{nd})/sin\theta_{dA})\}$ where u_{nd} is the unit vector normal to P_d, "x" represents the vector product operation and θ_{dA} is the angle between u_{nd} and u_{dA}. Note that θ_{dA} is equal to $arccos(\ u_{dA} * u_{nd})$ where "*" represents the scalar product operation. We now desire to find the contribution, df_j, of the normal and shear forces arising from dA to the total force f_j in the direction of an arbitrary unit direction vector u_j. Clearly this can be expressed as follows :

$$\begin{aligned} df_j &= \{s(dA)(u_{dA} \times u_{nd})/sin\theta_{dA}\} * u_j + p_{dA}(dA)u_{dA} * u_j \\ &= [s\{(dA \times u_{nd})/sin\theta_{dA}\} + p_{dA}dA] * u_j \end{aligned} \quad (2)$$

where dA is the area vector of the area element dA.

The total force f_j is obtained by integrating df_j over the entire area of the TLB, so that

$$f_j = [\int_{TLB}\{s(dA \times u_{nd})/sin\theta_{dA} + p_{dA}dA\}] * u_j \quad (3)$$

Note that in order to predict f_j from equation 3 we need to have a *complete* knowledge of the geometry of and the stress distribution on the TLB in addition to the orientation of vector u_{nd}. While it is recognised that such a complete knowledge concerning the TLB is probably impossible to obtain purely in terms of chip formation geometry, we will, in the next section, apply classical plasticity theory to the problem with a view to obtaining as much information concerning the TLB as possible with reasonable accuracy.

5. APPLICATION OF PLASTICITY THEORY

Consider now a cubic infinitesimal volume of material at an arbitrary point P on the TLB (see Fig. 2c). Let ψ_n be the angle between the plane tangent to the TLB at P and the cutting plane. Let η_s be the angular deviation of the shear velocity at point P from the normal plane, P_n, when measured in the plane tangential to the TLB at P. We choose the coordinate axes x, y and z at P as shown in Fig. 2c where axis x is parallel to the cutting edge, axis y is tangential to the TLB at P and lies in the normal plane and axis z is directed normal to the TLB at P. Then, following assumption A2, and applying classical plasticity theory we may write the following equations relating the normal stresses (σ values), shear stresses (τ values), velocities (V values) and strain rates (ϵ values) :

$$\frac{\tau_{xy}}{\dot{\epsilon}_{xy}}=\frac{\tau_{yz}}{\dot{\epsilon}_{yz}}=\frac{\tau_{xz}}{\dot{\epsilon}_{xz}}=\frac{\sigma_x-\sigma_m}{\dot{\epsilon}_x}=\frac{\sigma_y-\sigma_m}{\dot{\epsilon}_y}=\frac{\sigma_z-\sigma_m}{\dot{\epsilon}_z} \tag{4a-4e}$$

where

$$\sigma_m=\frac{1}{3}(\sigma_x+\sigma_y+\sigma_z),\quad \dot{\epsilon}_x=\frac{\partial V_x}{\partial x},\quad \dot{\epsilon}_y=\frac{\partial V_y}{\partial y},\quad \dot{\epsilon}_z=\frac{\partial V_z}{\partial z},$$
$$\dot{\epsilon}_{xy}=\frac{1}{2}\left(\frac{\partial V_x}{\partial y}+\frac{\partial V_y}{\partial x}\right),\quad \dot{\epsilon}_{yz}=\frac{1}{2}\left(\frac{\partial V_y}{\partial z}+\frac{\partial V_z}{\partial y}\right),\quad \dot{\epsilon}_{xz}=\frac{1}{2}\left(\frac{\partial V_z}{\partial x}+\frac{\partial V_x}{\partial z}\right) \tag{5a-5g}$$

From assumption A6, it follows that the velocity gradients ($\partial V_x/\partial x$, $\partial V_y/\partial x$ and $\partial V_z/\partial x$) along direction x parallel to the cutting edge must have zero magnitudes. Further, since the point under consideration is on the lower boundary of the primary deformation zone which must be a "shear surface", the velocity gradient $\partial V_z/\partial y$ must also have zero magnitude.
Thus,

$$\frac{\partial V_x}{\partial x}=\frac{\partial V_y}{\partial x}=\frac{\partial V_z}{\partial x}=\frac{\partial V_z}{\partial y}=0 \tag{6a-6d}$$

The assumption of thin primary deformation zone (assumption A7) implies that the velocity gradients across the thickness of the primary deformation zone (i.e. along z) must be substantially larger than those along its length (i.e. along y).
Thus,

$$\frac{\partial V_x}{\partial y},\frac{\partial V_y}{\partial y}<<\frac{\partial V_x}{\partial z},\frac{\partial V_y}{\partial z} \tag{7}$$

so that we may assume that $\partial V_x/\partial y\approx\partial V_y/\partial y\approx 0$. Combining this observation with equations 5 and 6, we have

$$\dot{\epsilon}_x=0,\quad \dot{\epsilon}_y\approx 0,\quad \dot{\epsilon}_{xy}\approx 0,$$
$$\dot{\epsilon}_{yz}=\frac{1}{2}\frac{\partial V_y}{\partial z},\quad \dot{\epsilon}_{xz}=\frac{1}{2}\frac{\partial V_x}{\partial z} \tag{8a-8e}$$

Further, combining equations 4, 5 and 8, we obtain

$$\sigma_x\approx\sigma_y\approx\sigma_z\approx\sigma_m,\quad \tau_{xy}\approx 0 \tag{9a-9d}$$

Again following the thin primary deformation zone assumption, we may further assume that

strain rate gradients ($\dot{\epsilon}_{xz}$, $\dot{\epsilon}_{yz}$) are uniformly distributed across the thickness (Δz) of the shear zone. The strain rate gradients can now be computed from known work and chip velocities as follows

$$\dot{\epsilon}_{xz} \approx \frac{1}{2}\frac{Vsini - V_c sin\eta_c}{\Delta z}$$
$$\dot{\epsilon}_{yz} \approx \frac{1}{2}\frac{Vcosi\ cos\psi_n + V_c cos\eta_c sin(\psi_n - \alpha_n)}{\Delta z} \qquad \text{(10a, 10b)}$$

Now combining equations 4 and 10, we have

$$\frac{\tau_{xz}}{\tau_{yz}} \simeq \frac{Vsini - V_c sin\eta_c}{Vcosi\ cos\psi_n + V_c cos\eta_c sin(\psi_n - \alpha_n)} \qquad \textbf{(11)}$$

From the definition of η_s and equation 11, it can be shown that

$$\tan\eta_s \approx \frac{\tau_{xz}}{\tau_{yz}} \qquad \textbf{(12)}$$

Equation 12 implies that, at any point on the TLB, the shear stress and the shear velocity are approximately collinear. Now we substitute equation 9 into Mises yield condition

$$(\sigma_x - \sigma_m)^2 + (\sigma_y - \sigma_m)^2 + (\sigma_z - \sigma_m) + 6(\tau_{xy}^2 + \tau_{yz}^2 + \tau_{xz}^2) = 6s^2 \qquad \textbf{(13)}$$

(where s is the flow stress of the unmachined work material) to obtain

$$\tau_{xz}^2 + \tau_{yz}^2 \approx s^2 \qquad \textbf{(14)}$$

Combining equation 14 with equation 12, we note that

$$\tau_{yz} \approx s\ cos\eta_s, \quad \tau_{xz} \approx s\ sin\eta_s \qquad \text{(15a, 15b)}$$

From Fig. 3, which shows how the stresses on a plane inclined at angle θ to plane xy (tangential to TLB) can be obtained from the equilibrium condition, we have

$$\tau_{y\theta} cos\theta - \sigma_\theta sin\theta + \sigma_y sin\theta + \tau_{yz} cos\theta = 0$$
$$\sigma_z cos\theta + \tau_{yz} sin\theta - \sigma_\theta cos\theta - \tau_{y\theta} sin\theta = 0 \qquad \text{(16a, 16b)}$$

However, we know that, on the surface of the uncut work material, the normal stress is of zero magnitude. Likewise, following assumption A6, we may assume that the shear stress in the plane normal to the tool cutting edge, P_n, is also of zero magnitude. Thus, letting $\sigma_\theta = \tau_{y\theta} = 0$, in equations 16a and 16b, we have

$$\sigma_z \approx -\tau_{yz},\ tan\theta^*, \qquad \sigma_y \approx -\tau_{yz}\ cot\theta^* \qquad \text{(17a, 17b)}$$

But from equation 9, $\sigma_z \approx \sigma_y$, so that

$$\psi_{nB} = \theta^* \approx 45^o \qquad \textbf{(18)}$$

where ψ_{nB} is the magnitude of ψ_n at the junction between the TLB and the unmachined work

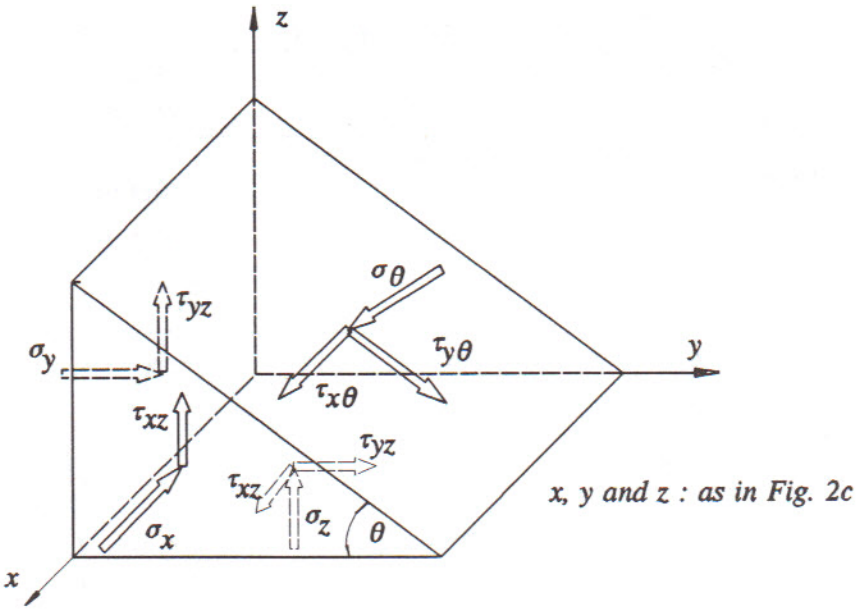

Fig. 4 Stresses on a Plane Inclined to the xy Plane at a Point on the TLB

surface. Equation 18 implies that the TLB meets the unmachined work surface at an angle approximately equal to 45°.

Finally, it follows from equations 15, 17 and 18 that the magnitude of the normal stress, p_B, on the TLB where it meets the unmachined work surface is given by

$$p_B = \sigma_z \text{ at } B \approx \tau_{yz} tan\psi_{nB} \approx \tau_{yz} \approx s \cos\eta_{sB} \tag{19}$$

where η_{sB} is the magnitude of η_s at the junction between the TLB and the unmachined work surface.

6. PREDICTION OF FORCE COMPONENTS PARALLEL TO THE CUTTING PLANE, P_s

We now know that it is reasonable to assume a uniformly distributed shear stress equal to s over the TLB. We also know that the normal stress on the TLB where it intersects the unmachined work surface is equal to ($s\ cos\eta_{sB}$). We will identify the exact method of computing η_{sB} later in this section. However, for the moment, we will assume that the magnitude of η_{sB} is known.

As in [4], we could assume that the normal stress on the portion, B'B"T"T, which is not coincident with the cutting plane, is uniformly distributed so that the magnitude of p_{dA} in equation 3 can be taken to be equal to ($s\ cos\eta_{sB}$) atleast over the non-coincident portion of the TLB (see curve b in Figure 4). However, there is considerable evidence in orthogonal cutting literature that the stresses in the primary deformation zone in the vicinity of the cutting edge are tensile whereas they are compressive elsewhere in the zone. Thus, one can expect that the actual normal stress distribution on the lower boundary is of the form characterised by curve a in Figure 4. In consequence, the mean normal stress, p, on the

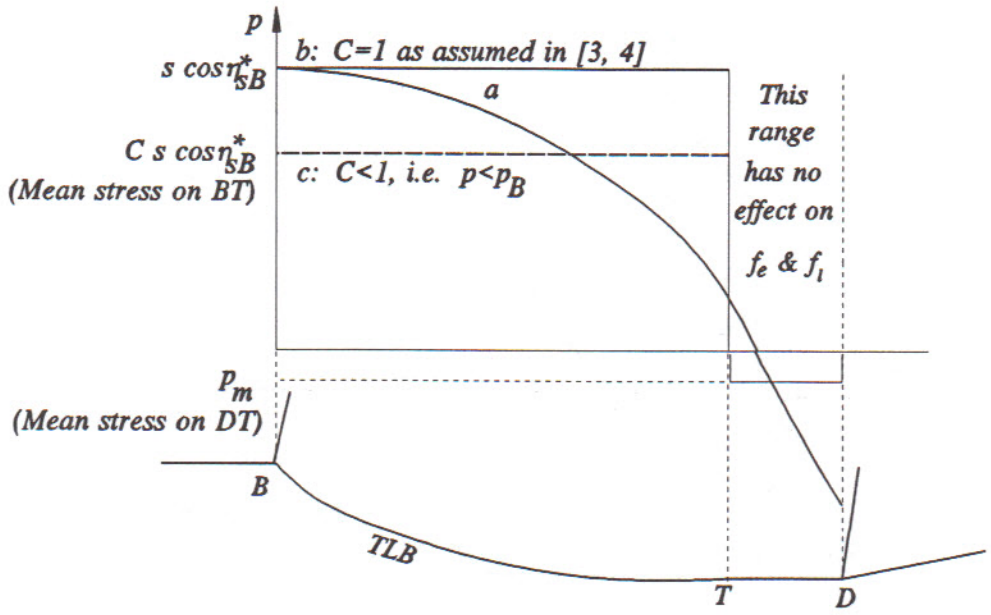

Fig. 4 Normal Stress Distribution on the TLB

non-coincident segment (B'B"T"T' in Figure 2 or BT in Figure 4) of the lower boundary could be different from the normal stress at the junction (B) with the unmachined surface. In particular, we may assume that the magnitude of p is a fraction C of the normal stress at B so that

$$p = C\ s\ cos\eta_{sB} \tag{20}$$

Equation 3 is still inadequate for estimating f_j since the geometry of the TLB which, strictly speaking, ought to be the path of integration is unknown. We will now explore the possibility of using an assumed path of integration. One candidate path consisting of two planes, namely planes 1 and 2, similar to the method adopted in orthogonal cutting [4] is illustrated in Fig. 2b. Here, plane 1 is inclined to the cutting plane, P_s, at an arbitrary angle ψ_{n1} whereas plane 2 is parallel to P_s. In order to enable force estimation from such an assumed path, equation 3 can be rewritten as

$$\begin{aligned} f_j &= [\sum_{k=1}^{2}\{s(A_k \times u_{nd})/sin\theta_k) + p_k A_k\}] * u_j \\ &= s\{(A_1 \times u_{nd})/sin\theta_1 + (A_2 \times u_{nd})/sin\theta_2 + C cos\eta_{sB} A_1\} * u_j + p_m(A_2 * u_j) \end{aligned} \tag{21}$$

where

- A_1 and A_2 are the area vectors of planes 1 and 2 in the assumed path of integration,
- p_1 and p_2 are the mean normal stresses on planes 1 and 2 respectively given by $p_1 = C\ s\ cos\eta_{sB}$ and $p_2 = p_m$ (of unknown magnitude),
- θ_1 and θ_2 are the angles between vectors A_1 and u_{nd}, and, between A_2 and u_{nd} respectively.

We note that equation 21 contains the parameter p_m of unknown magnitude. However, if we confine the prediction to a force component (such as f_l, f_{cn}, f_l or f_c) parallel to the cutting

plane, P_s, the term $A_2 * u_j$ will clearly vanish (since, by definition, A_2 is perpendicular to plane P_s while u_j is parallel to plane P_s) so that

$$f_j = s\{(A_1 \times u_{nd})/sin\theta_1 + (A_2 \times u_{nd})/sin\theta_2 + C\ cos\eta_{sB} A_1\} * u_j \quad : u_j \| P_s \qquad (22)$$

Equation 22 implies that the force estimate, f_j, is a function of the orientation of the deformation plane, P_d. More importantly, the presence of terms $sin\theta_1$ and $sin\theta_2$ in the equation implies that the reulting f_j estimate is path dependent, i.e. it depends on the prevailing geometry of the lower boundary of the primary deformation zone. In fact, it can be easily demonstrated that there is no deformation plane passing through V_s which results in the $sin\theta_1$ and $sin\theta_2$ terms vanishing from equation 22. It is therefore concluded that the condition that progressive deformation in the primary deformation zone should occur in a plane (see assumption A8) automatically precludes us from finding a path independent solution to oblique cutting. In contrast, if we allow the assumption that deformation could occur over a curved surface (still passing through V_s), it is possible that we could arrive at a path independent solution to the problem. However, such an analysis would require us to have the knowledge of the exact geometry of the TLB. Since we do not know the exact geometry of the TLB, we now examine the feasibility of finding an approximately path independent solution to the problem. We know from [4] that there exists a path independent solution to the problem when $i=0$. All that is required then is to find an acceptable deformation plane and check if the resulting errors are within acceptable limits. (It may be noted that in [5] Venuvinod had used a deformation plane normal to P_s.)

We now propose the "Effective Plane", P_{ef}, as a candidate for the deformation plane P_d, i.e. $P_d \equiv P_{ef}$. We base our arguments on intuition. Early metal cutting literature (in particular, [2]) had often invoked the effective plane in explaining some empirical observations from single edge oblique cutting. Shaw defines the effective plane, P_{ef}, as the plane parallel to the initial work velocity, V, as well as the final chip velocity, V_c. Note that this definition implies that P_{ef} is also parallel to V_s. Since the initial and final velocities of a work material element passing through the primary deformation zone are contained within P_{ef}, it is reasonable to assume that the entire progressive deformation of the element occurs within P_{ef}. Thus, replacing u_{nd} with the unit normal vector, u_{nef}, to P_{ef}, equation 22 can be rewritten as

$$f_j = s[\{(A_1/sin\theta_1)+(A_2/sin\theta_2)\} \times u_{nef} + C cos\eta^*_{sB}\ A_1] * u_j \quad : u_j \| P_s \qquad (23)$$

where η^*_{sB} is the magnitude of η_{sB} when P_d is taken parallel to P_{ef}; and θ_1 and θ_2 are the angles A_1 and u_{nef}, and, A_2 and u_{nef} respectively.

Equation 23 can be further simplified by noting and incorporating the following observations based on the geometry of chip formation :

- The area of Merchant shear plane, A_m, is given by

$$A_m = \frac{bt_1}{cosi\ sin\phi_n} \qquad (24)$$

- Since the bounding edges of the chain of planes 1 and 2 used in approximating the true lower boundary of the shear zone are common with those of the Merchant shear plane, we have

$$A_1 + A_2 = A_m = A_m u_m \tag{25}$$

where u_m is the unit vector normal to the Merchant shear plane, P_m.
(This is in fact true whatever the length of chain of planes used to approximate the TLB)

- From the definition of P_{ef} and the relative geometries of planes P_{ef} and P_m (Merchant shear plane) we note that

$$A_m \times u_{nef} / sin\theta_m = A_m(u_m \times u_{nef}) / sin\theta_m = A_m u_{Vs} \tag{26}$$

where u_{Vs} is the unit vector in the direction of the shear velocity vector, V_s, on the Merchant shear plane and θ_m is the angle between u_m and u_{nef}.

- We can estimate η_{sB}^* using the following equation :

$$\eta_{sB}^* = arctan\{\frac{tani\ cos(45^o - \alpha_n) - tan\eta_c\ sin45^o}{cos\alpha_n}\} \tag{27}$$

- We now arbtrarily assume that (we will examine later the error caused by this assumption)

$$A_1 / sin\theta_1 + A_2 / sin\theta_2 \approx A_m / sin\theta_m \tag{28}$$

- Since A_2 must be normal to P_s, we have $A_2 * u_j = 0$: $(u_j \parallel P_s)$ so that we can make the following vector transformations

$$Ccos\eta_{sB}^* A_1 * u_j = Ccos\eta_{sB}^*(A_1 + A_2) * u_j = Ccos\eta_{sB}^* A_m * u_j \quad : u_j \| P_s,\ A_2 \perp u_j \tag{29}$$

As a consequence of the above relationships, it can be shown that

$$f_j \approx sA_m\{(u_{Vs} * u_j) + Ccos\eta_{sB}(u_m * u_j)\} \quad : u_j \| P_s \tag{30}$$

Equation 30 provides an approximate but path independent solution to the problem of estimating f_j. The estimates of f_j obtained from equations 23 and 30 would clearly be identical when the TLB is identical to the Merchant shear plane. In practice, however, the TLB would deviate in geometry from the Merchant shear plane. Since the range of likely values of ψ_{nl} (the acute angle between P_s and plane A_1 with reference to equation 23) is ϕ_n to 45°, we may compute f_c and f_l estimates from equation 23 for this range of ψ_{nl} and compare them with the corresponding estimates from equation 30. When such a procedure was applied to the empirical data reported in [6] for machining aluminium alloy with single edge oblique tools, it was found that the force estimates were within $\pm 3\%$ of each other even when $i = 50^o$. For practical purposes, this is clearly an acceptable range of error.

Now taking u_j in equation 30 to be successively parallel to f_1, f_{cn}, f_l and f_c and evaluating the corresponding scalar products in terms of the geometric data set $\{i,\ \phi_n$ and $\eta_{sm}\}$ it can be shown that

$$f_1 \approx sA_m sin\eta_{sm} \tag{31}$$

$$f_{cn} \approx sA_m(cos\eta_{sm}\ cos\phi_n + C\ cos\eta_{sBef}\ sin\phi_n) \tag{32}$$

$$f_l = sA_m(cos\eta_{sm} cos\phi_n sini - sin\eta_{sm} cosi + Ccos\eta_{sBef} sin\phi_n sini) \tag{33}$$

$$f_c = sA_m(cos\phi_e + Ccos\eta_{sBef}sin\phi_n cosi) \quad (34)$$

where ϕ_e is the effective shear angle {$= arccos(V_s{*}V)$: shear angle measured in the efeective plane P_{ef}} is given by

$$\phi_e = arccos(cos\eta_{sm}cos\phi_n cosi + sin\eta_{sm}sini) \quad (35)$$

Note, when $i=0$ (and, therefore, $\eta_{sm}=0$), equation 34 reduces to the corresponding equation for orthogonal cutting (see equation 1). Thus, Rubenstein's solution to orthogonal cutting [4] is a specific case of the solution to oblique cutting developed here.

7. ESTIMATION OF THE THRUST FORCE COMPONENT, f_v

Equation 30 is not useful for estimating the thrust force component, f_v, because of the unknown magnitude of p_m which acts in the direction of f_v. However, if we assume that the condition of collinearity between V_c and the friction force at the chip/tool interface is obeyed, it is possible to derive the following equation for estimating f_v from the previously estimated magnitudes of f_l and f_{cn} which are not influenced by p_m (this condition and the following equation are implicit in the oblique cutting analyses described in [1,2 and 5])

$$f_v = f_l/(tan\eta_c cos\alpha_n) - f_{cn}tan\alpha_n \quad (36)$$

8. EXPERIMENTAL VERIFICATION OF THE NEW MODEL

We will now test the force predictions made in section 6 against experimental data. In particular we will use the data on single edge oblique cutting of an aluminium alloy, copper and mild steel presented in [6] and further experimental data (reproduced in Table 1) obtained by the present authors while cutting another aluminium alloy. The experimental procedure used in the further experiments was identical to that adopted in [7]. Chip thicknesses, chip flow angles and cutting forces were measured while dry cutting with a range of tool geometries (i = 0 to 50°, normal rake angle α_n=25 and 30°, t_1=0.05-0.175 mm). Edge forces were removed from the measured force components by the method used in [6] to yield the magnitudes of f_c and f_t.

On preliminary analysis none of the above data sets was found to satisfy the condition of collinearity between V_c and the friction force at the chip/tool interface. Hence, we will not attempt to test the prediction of f_v and confine our discussion to testing the prediction of force components parallel to the cutting plane, P_s. With this objective, the following procedure

Table 1. New Oblique Cutting Data While Machining Aluminum Alloy. (HSS Tool, Dry Cutting, Work Width 6mm)

t_1 (mm)	i (deg)	Normal rake 25°					Normal Rake 30°				
		Φ_n (deg)	η_c (deg)	f_c (N)	f_l (N)	f_v (N)	Φ_n (deg)	η_c (deg)	f_c (N)	f_l (N)	f_v (N)
.050	0	31.4	0	169	0	29	35.5	0	174	0	19
.075	0	32.0	0	269	0	49	35.5	0	254	0	29
.100	0	34.0	0	329	0	54	35.5	0	334	0	39
.125	0	33.0	0	429	0	74	35.5	0	424	0	49
.150	0	33.0	0	519	0	89	35.5	0	494	0	54
.175	0	35.1	0	599	0	104	35.5	0	604	0	69
.050	10	32.0	10	193	16	20	35.5	11	145	20	16
.075	10	35.1	10	263	26	45	35.5	12	245	30	27
.100	10	33.0	10	343	26	60	36.6	11	320	40	37
.125	10	34.0	9	463	36	80	36.6	11	420	50	47
.150	10	34.0	9	543	46	85	37.7	10	460	60	52
.175	10	35.1	10	633	56	90	37.7	10	550	70	62
.050	20	33.0	18	166	53	17	37.7	18	183	38	22
.075	20	34.0	20	236	68	27	37.7	20	253	53	34
.100	20	35.1	20	336	88	37	37.7	16	338	88	44
.125	20	35.1	24	436	108	52	38.8	20	418	88	52
.150	20	35.1	16	506	138	57	38.8	19	498	103	64
.175	20	35.1	21	566	168	62	38.2	18	618	128	79
.050	30	34.0	30	191	55	29	37.7	30	141	50	9
.075	30	35.1	30	261	75	44	37.7	33	236	67	21
.100	30	36.1	32	341	95	59	37.7	28	316	92	23
.125	30	37.1	34	401	115	69	37.7	27	386	117	26
.150	30	38.1	36	521	150	84	37.7	27	446	137	31
.175	30	37.1	34	631	180	104	37.7	29	536	167	41
.050	40	35.1	35	217	87	21	37.7	40	151	63	4
.075	40	36.1	36	297	122	41	38.8	38	276	116	14
.100	40	37.1	44	407	152	66	38.8	36	361	151	14
.125	40	37.1	37	497	192	66	38.8	36	436	173	19
.150	40	38.1	36	647	242	106	38.8	39	521	218	21
.175	40	38.1	37	707	287	81	38.8	36	596	248	24
.050	50	37.1	45	164	75	2	40.9	46	195	106	-4
.075	50	38.1	51	299	190	12	40.9	46	220	116	-1
.100	50	39.1	48	299	190	12	39.8	52	350	176	-1
.125	50	40.1	46	444	270	7	39.8	47	400	211	-1
.150	50	40.1	50	529	310	17	40.9	47	500	261	-6
.175	50	41.0	44	659	375	17	40.9	47	605	321	-6

Note: The forces reported are obtained after removing edge forces.

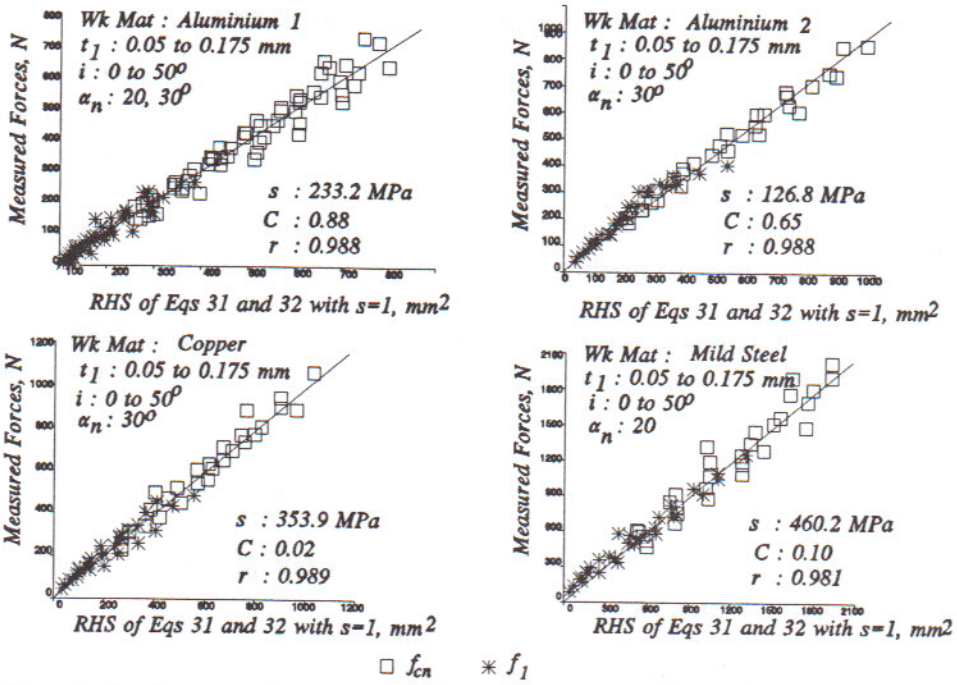

Fig. 5 Correlation Between Forces as Predicted by Equation 30 and Measured Forces

Table 2 Results Obtained from the Application of the TLB Model to Experimental Data

work material	s (Mpa)	C	Correlation Coefficient, r	Data from Reference
Aluminium Alloy 1	233.2	0.88	0.988	new data
Aluminium Alloy 2	126.8	0.65	0.988	7
Copper	353.9	0.02	0.989	7
Mild Steel	460.2	0.10	0.981	7

is applied with respect all the data obtained while machining each work material :

- Firstly, the magnitudes of A_m and η_{sB}^* are computed using equations 24 and 27 respectively.
- The magnitudes of f_1 and f_{cn} are estimated from the measured f_t and f_c as

$$f_1 = f_c sini - f_t cosi \quad (37)$$

$$f_{cn} = f_c cosi + f_t sini \quad (38)$$

- Next, a linear regression is performed with the coefficient of s in equation 31 taken along the x axis and f_1 along the y axis such that the resulting regression line has zero y intercept. The slope of the regression line will then give the estimate of the shear flow stress, s, on the TLB.
- Next, equation 32 is rearranged as

$$f_{cn} - sA_m cos\eta_s cos\phi_n = CsA_m cos\eta^*_{sB} sin\phi_n \quad (39)$$

so that the magnitude of C may be estimated by a similar regression between the coefficient of C and the magnitude of the term on the left hand side of this equation. (It may be noted that the hypothesis that the magnitude of C is a material constant is implicit in this procedure.)

- Next, the magnitudes of s and C thus obtained are assumed to be constant for a given work material and used to predict f_t, f_{cn}, f_l and f_c from equations 31 to 34 respectively.

Figure 5 shows the correlation between the predicted and actual magnitudes of f_t and f_{cn} for the four different work materials used in the tests. Table 2 summarises some key results.

The following conclusions may be drawn from these results :

- The correlation between predicted and actual force components is excellent when the optimum magnitude of C is used.
- The magnitudes of s and C are found to be constant for a given work material despite the wide range of obliquities and uncut chip thickenesses (and some variation in the rake angle) covered by the tests. This means that the new model of oblique cutting enables the prediction of forces parallel to the cutting plane purely from a prior knowledge of material dependent parameters s and C, and a knowledge of tool and chip geometry. Note further that the new model, unlike models based on Merchant shear plane, does not presuppose any knowledge of friction conditions at the chip/tool interface.
- A detailed examination of the data obtained at each cutting condition has shown that the magnitude of C is quite sensitive to variation (or error) in η_c. Further, it appears that C cannot be evaluated with confidence purely from orthogonal cutting data (this might explain why Rubenstein did not identify the role of C in [3]). A consequence of these observations is that C needs to be determined from oblique cutting data itself which, at first glance, appears to contradict the claim that the proposed model is capable of predicting forces in oblique cutting. However, since the magnitude of C is insensitive to changes in t_1 and i (and, to some extent, changes in the rake angle), it is possible to determine the magnitudes of s and C from a limited set of oblique cutting experiments and the values so obtained used to predict cutting forces at all other oblique cutting conditions.
- From the magnitudes of C as listed in Table 2 for different work materials, it is seen that the normal stress distribution on the TLB tends to be significantly more non-uniform (tending towards more tensile stresses) for copper and mild steel than for aluminium alloy. Further research is needed to confirm this observation and understand its full implications.

9. CONCLUSIONS

A new analysis of single edge oblique cutting based on a model of the geometry of and stress distributions on the true lower boundary of the primary deformation zone has been presented above. Equation 30 may be used to predict the force components parallel to the cutting plane with reasonable accuracy from a knowledge of the flow stress, s, of the work material, the uncut area, the chip thickness and the chipflow angle. Further, the thrust force component, f_v, can be predicted provided the principle of collinearity between the tangential stress and

tangential velocity at the tool/chip interface is satisfied. It however turns out that such collinearity is rarely obtained in empirical data on oblique cutting. Further research is needed to resolve this problem.

The model is an improvement over previous attempts aimed at extending Rubenstein's approach to modelling orthogonal cutting [3,4] to the case of oblique cutting. As noted earlier, models based purely on the Merchant shear plane , such as in [1,2], have no ability to predict any of the cutting force components. The model developed in [7], although capable of predicting the cutting forces, does not attempt to model the actual TLB in oblique cutting. Instead, it relies on the concept of equivalent orthogonal cutting to enable the utilisation of a TLB based solution to orthogonal cutting. Further, this model requires that not only the flow stress, s, of the uncut material but also the shear stress, τ, on the Merchant shear plane be taken as a material constant. These aspects diminish the elegance of this approach. The model developed in [5] relies on an intuitive idealisation of the TLB in oblique cutting and lacks the rigour of the present approach. Further, the predictive ability of this model in terms of f_l is not satisfactory.

The new model has demonstrated a rigorous and direct approach to the modelling of TLB in oblique cutting. In particular, it has attempted to systematically extend the fundamental notions contained in Rubenstein's TLB based model for orthogonal cutting [3 and 4] to the three dimensional situation prevailing in oblique cutting. The goal of achieving an exact and path independent solution to oblique cutting, however, continues to elude us.

The present work has observed that it is important to recognise the significance of the non-uniformity of the normal stress distribution on the TLB. This aspect was left unaddressed in the original orthogonal cutting model [3 and 4]. Further research is needed to investigate the full implications of this observation.

ACKNOWLEDGEMENT

The authors wish to thank the City Polytechnic of Hong Kong for the financial support (Strategic Research Grant 781) provided for this work. We also acknowledge the contributions made by Mr C.M. Lee, a research student working under the supervision of the first author, to some preliminary modelling work and in obtaining the new oblique cutting data reported in this paper.

REFERENCES

[1] M.E. Merchant, Basic Mechanics of the Metal Cutting Process, *J. appl. Mech.* **66**,A168 (1944).

[2] M.C.Shaw, Metal Cutting Principles, 3rd Ed., M.I.T. Press, Cambridge, Mass. (1957).

[3] R. Connolly and C. Rubenstein, The Mechanics of Continuous Chip Formation in Orthogonal Cutting, *Int. J. Mach. Tool Des. Res.* **8**, 159-187 (1968).

[4] C. Rubenstein, The Application of Force Equilibrium Criteria to Orthogonal Cutting, *Int. J. Mach. Tool Des. Res.* **12**, 121-126 (1972).

[5] P.K. Venuvinod and W.S. Lau, On a New Model of Oblique Cutting, *Trans. Am. Soc. Mech. Engrs, J. Eng. Ind.* **100**, 287-292 (1978).

[6] W.S. Lau and C. Rubenstein, The Mechanics of Continuous Chip Formation In Oblique Cutting in the Absence of Chip Distortion. Part 2 - Comparison of Experimental Data with Deductions from Theory, Int. J. Mach. Tool Des. Res., 23, 1, 21-37 (1983).

[7] Rubenstein, The Mechanics of Continuous Chip Formation in Oblique Cutting in the Absence of Chip Distortion. Part 1 - Theory, *Int. J. Mach. Tool Des. Res.* **23**, 1, 11-20 (1983).